Peripheral elevation of TNF-α leads to early synaptic abnormalities in the mouse somatosensory cortex in experimental autoimmune encephalomyelitis

Guang Yang[a,b,1,2], Christopher N. Parkhurst[a,1], Scott Hayes[a,b,1], and Wen-Biao Gan[a,2]

[a]Molecular Neurobiology Program, Skirball Institute, Department of Physiology and Neuroscience, New York University School of Medicine, New York, NY 10016; and [b]Department of Anesthesiology, New York University School of Medicine, New York, NY 10016

Edited by Marc Feldmann, University of Oxford, London, United Kingdom, and approved May 13, 2013 (received for review December 31, 2012)

Sensory abnormalities such as numbness and paresthesias are often the earliest symptoms in neuroinflammatory diseases including multiple sclerosis. The increased production of various cytokines occurs in the early stages of neuroinflammation and could have detrimental effects on the central nervous system, thereby contributing to sensory and cognitive deficits. However, it remains unknown whether and when elevation of cytokines causes changes in brain structure and function under inflammatory conditions. To address this question, we used a mouse model for experimental autoimmune encephalomyelitis (EAE) to examine the effect of inflammation and cytokine elevation on synaptic connections in the primary somatosensory cortex. Using in vivo two-photon microscopy, we found that the elimination and formation rates of dendritic spines and axonal boutons increased within 7 d of EAE induction—several days before the onset of paralysis—and continued to rise during the course of the disease. This synaptic instability occurred before T-cell infiltration and microglial activation in the central nervous system and was in conjunction with peripheral, but not central, production of TNF-α. Peripheral administration of a soluble TNF inhibitor prevented abnormal turnover of dendritic spines and axonal boutons in presymptomatic EAE mice. These findings indicate that peripheral production of TNF-α is a key mediator of synaptic instability in the primary somatosensory cortex and may contribute to sensory and cognitive deficits seen in autoimmune diseases.

Sensory, motor, and cognitive dysfunctions are common at the early stages of autoimmune diseases, including in more than half of multiple sclerosis (MS) patients (1–5). The increased production of proinflammatory cytokines and infiltration of peripheral immune cells into the central nervous system (CNS) are closely associated with neuronal damage in the spinal cord and many brain regions (6–10). Elevation of several cytokines such as TNF-α and IFN-γ precedes infiltration of peripheral immune cells and could have a significant impact on neuronal function (11–19), potentially contributing to early sensory and cognitive impairments. However, the link between the cytokine elevation and CNS deficits in autoimmune diseases remains unclear.

Experimental autoimmune encephalomyelitis (EAE) is a commonly used animal model to study the pathogenesis and treatment of MS (20). Previous studies have shown early behavioral changes, including decreased exploratory behavior and increased startle response before the onset of paralysis in EAE mice (21). The mechanisms underlying these early behavioral changes remain to be addressed. In EAE, activated antigen-specific T cells migrate through the blood brain barrier (BBB) and subsequently recruit additional myeloid and lymphoid cells to the spinal cord and susceptible brain regions (22–24). The resulting inflammatory cascade eventually leads to axonal loss and neuronal death. However, inflammatory infiltrates usually accompany the onset of clinical EAE and are therefore unlikely to contribute to sensory and behavioral deficits in presymptomatic mice. On the other hand, elevation of proinflammatory cytokines occurs during the early phase of EAE induction (25). Cytokines such as TNF-α are produced by activated cells within peripheral lymphoid tissues as well as by CNS-resident microglia in response to a number of inflammatory stimuli. Peripherally produced TNF-α can enter the circulation and cross the BBB through active transport (26–28) or passively after pathologic BBB disruption (27, 29). TNF-α has been shown to affect synaptic transmission and synaptic scaling (30–32), as well as regulate the production of other cytokines and chemokines to impact neuronal function. The induction and progression of EAE can be inhibited by either i.p. or intracranial injection of anti-TNF antibodies (33). Therefore, TNF-α elevation under pathological conditions could cause significant deficits in the CNS and contribute to behavioral abnormalities in EAE.

TNF-α is known to affect neuronal functions by acting at two receptor types, TNF receptor (TNFR)1 and TNFR2, each having divergent effects in the CNS (16, 34). TNFR2 responds mainly to transmembrane TNF-α, which is thought to be a prosurvival signal. In contrast, TNFR1 responds mainly to circulating soluble TNF-α (solTNF) and plays a role in inflammation, proliferation, and neural migration. Activation of TNFR1 has been found to affect synaptic scaling by recruiting AMPA receptors to the postsynaptic cell membrane (30–32). TNFR1 activation also initiates the JNK pathway thought to be involved in dendritic cytoskeleton stability via regulation of microtubules (16). A dominant negative TNF inhibitor, XPro1595, blocks the effects of solTNF to selectively decrease the activation of TNFR1 (35, 36). Recently, decreased activation of TNFR1 via XPro1595 has been shown to promote axonal integrity and improve clinical outcome of mice with EAE (10).

In this study, we examined the changes in synaptic connections in the primary somatosensory cortex in response to inflammation in an EAE mouse model. Using transcranial two-photon microscopy (37, 38), we followed postsynaptic dendritic spines and presynaptic axonal boutons over time in mice immunized with myelin oligodendrocyte glycoprotein peptide ($MOG_{35–55}$). We found that, in conjunction with an elevation of peripheral TNF-α production, the turnover of dendritic spines and axonal boutons was significantly increased in the cortex within 7 d of MOG immunization, several days before the onset of paralysis. The turnover of dendritic spines and axonal boutons continued to increase as the disease progressed. This early instability of cortical synaptic connections in EAE mice is independent of T-cell infiltration and microglia activation, but depends on the elevation of peripheral TNF-α in EAE mice.

Author contributions: G.Y., C.N.P., S.H., and W.-B.G. designed research; G.Y., C.N.P., and S.H. performed research; G.Y., C.N.P., and S.H. analyzed data; and G.Y., C.N.P., S.H., and W.-B.G. wrote the paper.

The authors declare no conflict of interest.

This article is a PNAS Direct Submission.

[1]G.Y., C.N.P., and S.H. contributed equally to this work.

[2]To whom correspondence may be addressed. E-mail: gan@saturn.med.nyu.edu or guang.yang@nyumc.org.

Results

Dendritic Spine Turnover Increases in the Somatosensory Cortex of EAE Mice. To investigate whether alterations of cortical synapses occur in the early stages of EAE, we imaged postsynaptic dendritic spines of layer V pyramidal neurons in the somatosensory cortex before $MOG_{35–55}$ immunization (day 0) and 7 d after immunization (Fig. 1*A*). We found that none of the MOG-immunized mice displayed clinical symptoms of EAE by 7 d post-immunization, whereas most MOG-immunized mice began to exhibit signs of paralysis by day 10, and 100% by day 14 (Fig. 1*B*). In contrast, the Mock control mice that received injections of complete Freund's adjuvant (CFA) and pertussis toxin but without MOG peptide showed no clinical symptoms by day 14 (Fig. 1*B*). Notably, within the first 7 d, there was a significant increase in the elimination and formation rates of dendritic spines in EAE mice (elimination: 10.8 ± 1.0%; formation: 8.8 ± 1.3%, 976 spines, five animals; Fig. 1 *A–H*), compared with either the no-injection control or the Mock control. Consistent with previous studies (39), the vast majority of dendritic spines persisted over 7 d in the no-injection control mice (elimination: 4.3 ± 0.5%; formation: 4.0 ± 0.5%, 636 spines, four animals). No significant difference in spine turnover was found between the no-injection and the Mock control mice ($P > 0.08$). These results indicate that MOG immunization leads to abnormally high turnover of post-synaptic dendritic spines in the somatosensory cortex before the onset of paralysis.

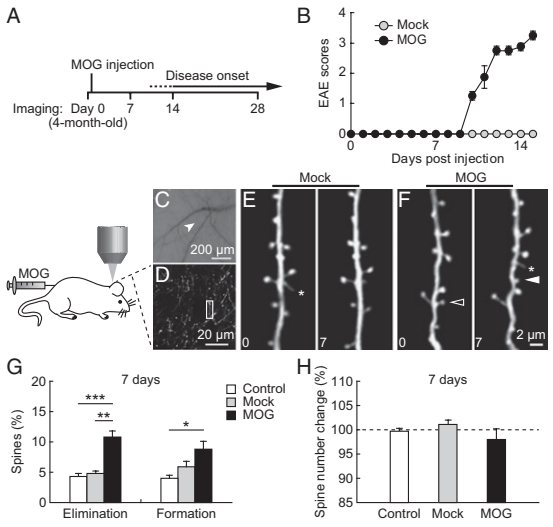

Fig. 1. Increased spine turnover before the onset of paralysis in MOG-EAE mice. (*A*) Schematic diagram of the experiment. (*B*) Clinical scores of mice with MOG-induced EAE. Four-month-old adult mice were immunized by $MOG_{35–55}$ on day 0. Clinic symptoms began at days 10–15 postimmunization. No mice showed disease symptoms before day 7. (*C*) CCD camera view of the vasculature of the somatosensory cortex below the thinned skull. The arrow indicates the region where the two-photon image in *D* was obtained. (*D*) Low-magnification image of apical dendrites of layer V pyramidal neurons. A higher-magnification view of the dendritic segment (box in *D*) is shown in *F*. (*E* and *F*) Repeated imaging of dendritic branches over 7 d in the cortex of Mock- and MOG-immunized animals. Filled and empty arrowheads indicate spines that were formed and eliminated between the two views. Asterisks indicate filopodia. (*G*) Percentage of spines eliminated and formed over 7 d in no-injection control, Mock-immunized, and MOG-immunized animals. A significant increase in both spine elimination and formation was found in MOG-immunized animals compared with no-injection control and Mock-immunized animals. (*H*) The total number of spines remains the same over 7 d in all groups of animals. Data are presented as mean ± SEM. $*P < 0.05$; $**P < 0.01$; $***P < 0.001$.

To further determine synaptic alterations as EAE progresses, we examined the elimination and formation rates of dendritic spines over 14 and 28 d after EAE induction (Fig. 1*A*). We found that spine elimination and formation continued to increase in the clinical phase of EAE (Fig. 2). Over 14 d, 14.6 ± 1.8% of spines were eliminated and 12.0 ± 0.4% of spines were formed in MOG-immunized mice, whereas only 7.2 ± 1.4% of spines were eliminated and 7.7 ± 1.0% of spines were formed in Mock-immunized mice ($P < 0.05$; Fig. 2*A*). This elevated spine turnover was sustained over 28 d in EAE mice (elimination: 19.6 ± 1.5%; formation: 16.3 ± 3.9%; Fig. 2*B*). Although there was no significant difference in spine turnover over 7 d between the no-injection control and the Mock control mice, the spine turnover of Mock-immunized mice was significantly higher than that of the no-injection control over 14 and 28 d ($P < 0.05$), suggesting that CFA and/or pertussis toxin also affect the dynamics of synapses over the long term. We did not observe significant changes of total spine number within the first month after EAE induction (Fig. 2 *C* and *D*).

Axonal Bouton Turnover Increases in the Cortex of EAE Mice. To further investigate synaptic alterations in EAE mice, we analyzed the dynamics of axonal boutons before and after the onset of paralysis. Previous studies have shown that the majority of axonal boutons are in contact with postsynaptic structures (40). Consistent with the increased dendritic spine turnover after EAE induction, we found a significant increase in the dynamics of axonal boutons as early as 7 d post-MOG immunization compared with the no-injection control and the Mock-immunized control. Over 7 d, 4.4 ± 0.5% of boutons were eliminated and 5.5 ± 0.9% were formed in EAE mice whereas only 2.3 ± 0.5% of boutons were eliminated and 2.3 ± 0.5% were formed in Mock-immunized mice ($P < 0.05$, Fig. 3 *A* and *B*). The elimination and formation of axonal boutons continued to increase in EAE mice in comparison with Mock control after the disease onset ($P < 0.05$). Over 14 d, 6.5 ± 0.9% of boutons were eliminated and 6.4 ± 0.7% were formed in EAE mice, whereas only 3.5 ± 0.6% of boutons were eliminated and 3.5 ± 0.9% were formed in Mock-immunized controls (Fig. 3*C*). Elevated turnover of axonal boutons was sustained through the first month after EAE induction (Fig. 3*D*).

Absence of T-Cell Infiltration and Microglial Activation in Presymptomatic EAE Mice. To determine whether T-cell infiltration is involved in the synaptic structural instability in the cortex of presymptomatic EAE mice, we examined the CNS for the presence of $CD4^+$ or $CD8^+$ cells at day 7 postimmunization. We observed no increase in either population in the CNS of presymptomatic EAE mice (Fig. 4 *A* and *B*), suggesting that T-cell infiltration is unlikely to be responsible for the early synaptic instability. Activation of microglia has been previously reported to occur around the onset of clinical EAE symptoms within specific brain regions (41). To determine whether microglial activation occurs early in the somatosensory cortex, we first examined Iba-1^+ (ionized calcium-binding adaptor molecule 1) microglia for evidence of histological change within the primary somatosensory cortex at day 7 postimmunization. There was no detectable change in the number or morphology of Iba-1^+ cells in MOG-immunized animals compared with Mock-immunized controls (Fig. 4 *C* and *D*). We next examined changes in immunological markers characteristic of activation in both microglial and non-microglial CNS myeloid populations at day 7 postimmunization (Fig. 4 *E* and *F*). No increase in the levels of MHC II, CD80, or CD86 was observed in either the nonmicroglial ($CD11b^+$ CX_3CR1^{int}) myeloid population or the microglial ($CD11b^+$ CX_3CR1^{hi}) population in MOG-immunized animals compared with Mock-immunized controls. Taken together, these results suggest that T-cell infiltration and microglial activation are absent

NEUROSCIENCE

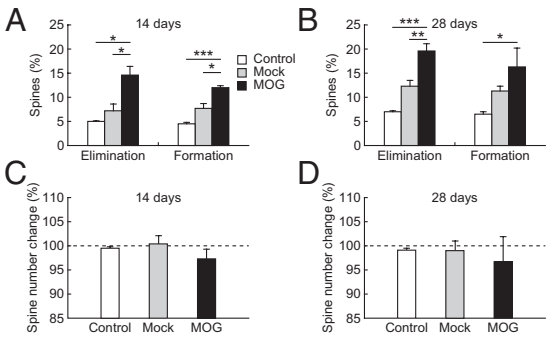

Fig. 2. Spine turnover in the cortex continually increased during EAE progression. (*A* and *B*) Percentage of spines eliminated and formed over 14 d (*A*) and 28 d (*B*) in no-injection control, Mock-immunized, and MOG-immunized animals. A significant increase in both spine elimination and formation was found in MOG-immunized animals compared with no-injection control and Mock-immunized animals. (*C* and *D*) No significant change in total spine number was observed over 14–28 d in all animal groups. Data are presented as mean ± SEM. $*P < 0.05$; $**P < 0.01$; $**P < 0.001$.

at day 7 postimmunization and therefore are unlikely to account for early synaptic alterations in the somatosensory cortex.

Peripheral Production of TNF-α Is Important for Early Synaptic Alteration. The initiating events in EAE induction require antigen presentation and clonal T-cell expansion within peripheral lymphoid tissues including the draining lymph nodes (42). Accompanying these events is an increase in the production and circulation of numerous cytokines including TNF-α. It has been shown that the expression of the cytokines in brain tissue increases during EAE onset and decreases during the recovery phase (25). Because TNF-α has been shown to have significant effects on synaptic functions (28), we assayed for increased protein and mRNA levels of TNF-α in both the CNS and peripheral lymphoid tissues at days 7, 14, and 28 postimmunization. At day 7 postimmunization, a significant increase in TNF-α protein was observed in both the serum and the CNS of MOG-immunized animals compared with the Mock controls (Fig. 5 *A* and *B*). On the other hand, elevated TNF-α mRNA levels rose significantly in the draining lymph nodes and spleen of MOG-immunized animals, but not in CNS tissues at day 7 (Fig. 5 *C–E*). At day 14 postimmunization, TNF-α mRNA and protein levels were significantly elevated in both peripheral and CNS tissues (Fig. 5 *A–E*). By day 28 postimmunization, TNF-α mRNA and protein were significantly elevated only in CNS tissues. Taken together, these results indicate that during the period of early synaptic alteration (day 7 postimmunization) TNF-α is produced in the peripheral lymphatic tissues, but can be found in the circulation and within the CNS. The production and distribution of TNF-α change at later time points with a shift from peripheral to CNS tissues by day 28 postimmunization.

To investigate whether the observed peripheral elevation of TNF-α is important for synaptic alterations in the somatosensory cortex, we examined the effect of chronic inhibition of TNF-α on dendritic spine and axonal bouton plasticity by applying a dominant negative form of TNF-α (DN-TNF) for 1 wk (10 mg/kg body weight, 1–2 times per day) after MOG immunization. DN-TNF selectively decreases activation of TNFR1 by blocking the effects of circulating soluble TNF-α (35, 36). This inhibition resulted in a significant reduction in the rate of spine elimination and formation in MOG-immunized mice (elimination: 4.6 ± 0.6%; formation: 4.8 ± 0.7%, 743 spines, five animals) (Fig. 5*F*). The elevated turnover of axonal boutons over the first week post-MOG immunization was also reduced in DN-TNF–treated animals (elimination: 2.9% ± 0.1%; formation: 2.7% ± 0.4%; 482 boutons, five animals; Fig. 5*G*). These results indicate that peripheral elevation of TNF-α has a critical role in early synaptic alterations in EAE mice.

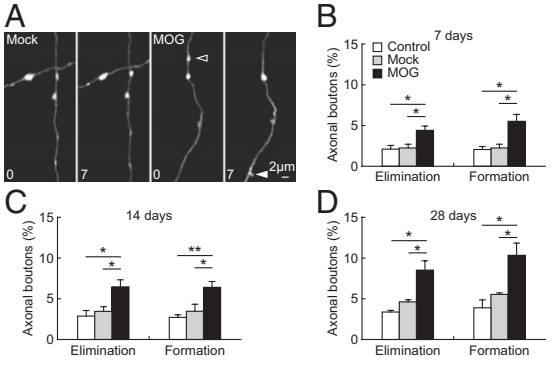

Fig. 3. Increased turnover of axonal boutons after MOG immunization. (*A*) Repeated imaging of axonal segments in the somatosensory cortex over 7 d in Mock- and MOG-immunized animals (4-mo-old). Filled and empty arrowheads indicate axonal boutons that were formed and eliminated between the two views. (*B–D*) Percentage of axonal boutons eliminated and formed over 7 d (*B*), 14 d (*C*), and 28 d (*D*) in no-injection control, Mock-immunized, and MOG-immunized animals. The turnover of axonal boutons was significantly increased in MOG-immunized animals compared with no-injection and Mock-immunized control in all of the time intervals. Data are presented as mean ± SEM. $*P < 0.05$; $**P < 0.01$.

Discussion

Our study demonstrates that peripheral TNF-α production in preclinical EAE readily causes instability of synaptic connections in the cortex. Using in vivo two-photon microscopy, we observed increased turnover of both postsynaptic dendritic spines and presynaptic axonal boutons in the somatosensory cortex of presymptomatic EAE mice. These early alterations of synaptic structural dynamics were observed in conjunction with increased peripheral lymphoid TNF-α production and in the absence of increased production in CNS tissues or microglial activation. Peripheral administration of a soluble TNF inhibitor blocked the abnormal plasticity of dendritic spines and axonal boutons observed in presymptomatic EAE mice, suggesting that TNF-α plays a crucial role in inflammation-mediated changes in synaptic connections in the sensory cortex.

Previous studies have shown that the majority of dendritic spines persist in the adult cortex and are likely essential for information processing and memory storage (43, 44). The abnormally high turnover of cortical connections suggests the disruption of stably maintained synaptic networks, which likely contributes to impaired cortical function. Consistent with this notion, EAE mice display behavioral changes early in the disease course, before the onset of paralysis. Previous research has described an EAE-associated behavioral syndrome, including reduced consumption of sucrose solution, decreased exploratory behavior, and increased startle response occurring several days before the onset of clinical motor symptoms (21). Furthermore, EAE shares many pathological features with MS (20). Patients with MS, even at early stages of the disease, have been shown to have sensory deficits (1–5) and decreased performance on memory tasks with changes in cortical functional MRI activity levels (45). Thus, the early synaptic abnormalities observed in our studies may similarly occur in MS and contribute to the early cortical deficits. In addition, persistent synaptic alterations observed in the cortex of EAE mice may have important implications for the study of human MS as gray matter pathology in both diseases appears to be independent of T-cell infiltration (46). Future studies are needed to investigate how the elevation of cytokines and other

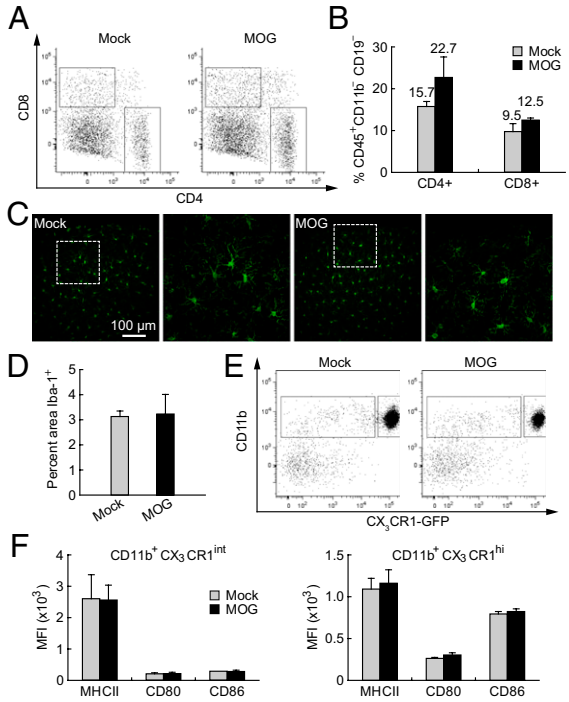

Fig. 4. Absence of peripheral T-cell infiltration and microglia activation in CNS within 7 d after MOG immunization. (*A*) Flow cytometric data from homogenized brains of Mock- and MOG-immunized mice. The left and right boxes indicate $CD8^+$ and $CD4^+$ populations, respectively. (*B*) Percentage of $CD45^+$ $CD11b^-CD19^-$ cells in the $CD4^+$ and $CD8^+$ gates. There is no significant difference between Mock- and MOG-immunized mice ($P > 0.5$). (*C*) Microglia morphology in the cortex was shown by immunolabeling for Iba-1. There is no obvious difference in microglia morphology between Mock- and MOG-immunized animals at day 7 postimmunization. (*D*) No significant difference in the area covered by Iba-1^+ microglia between Mock- and MOG-immunized animals at day 7 ($P > 0.9$). (*E*) The nonmicroglial myeloid population (left box: $CD11b^+$ CX_3CR1^{int}) and the microglial population (right box: $CD11b^+$ CX_3CR1^{hi}) were determined by FACS analysis from the homogenized brain. (*F*) There was no significant increase in the levels of MHC II, CD80, or CD86 in either the nonmicroglial myeloid population or the microglial population in MOG-immunized animals compared with Mock-immunized controls at day 7 postimmunization ($P > 0.3$).

factors including microglial activation contribute to cortical damage at specific stages of EAE and MS.

Although T-cell infiltration is a necessary event for EAE-induced CNS demyelination (23), destabilization of synaptic connections in the cortex was initiated in the absence of T-cell infiltration or microglial activation. Instead, we found that, accompanying early alterations in synaptic structural plasticity, TNF-α production was increased in peripheral lymphoid, but not CNS tissues. Blocking soluble TNF-α with DN-TNF prevented cortical synaptic instability in EAE mice. Peripherally produced TNF-α can cross the BBB through active transport (26–28), and TNF transporters have been identified on BBB endothelial cells (28). Additionally, TNF-α may also passively cross the BBB due to pathologic BBB disruption in EAE (27, 29). Once in the brain, TNF-α may affect synaptic plasticity directly through TNFR1 at cortical neurons to increase synaptic plasticity. TNF-α is known to affect dendrite morphology via the modulation of NF-κB (47) and modify synaptic strength via increased expression of AMPA receptors (31). TNF-α has also been shown to trigger the release of brain-derived neurotrophic factor, which is a potent regulator of synaptic plasticity (48–50). Furthermore, inhibiting soluble TNF-α decreases downstream expression of IFN-γ, IL-1β, IL-6, or CCL2 [chemokine (C-C motif) ligand 2] in the periphery (10). Because IFN-γ and IL1-β are important regulators of neuronal functions (51), selectively blocking soluble TNF-α activity with DN-TNF may indirectly affect synaptic plasticity by regulating the production of other cytokines. Finally, TNF-α signaling through TNFR1 is required for vascular cell adhesion molecule 1 expression on astrocytes and could play an important role in facilitating the infiltration of effector T cells into the CNS parenchyma and causing subsequent neuronal damage in EAE (52, 53). The detailed mechanisms underlying the effect of TNF-α on cortical synaptic plasticity at different stages of EAE remain to be determined.

The effect of cytokines such as TNF-α on the cortex may play a broad role in neuropathology. High serum levels of TNF-α are associated with neuropsychiatric disorders such as major depressive disorder (11, 54), abnormalities of brain development including autism (55), autoimmune diseases such as multiple sclerosis and rheumatoid arthritis (56), postoperative cognitive decline (57), and neurodegenerative diseases such as Alzheimer's disease (58). High serum cytokine levels in patients immunized with lipopolysaccharide or *Salmonella typhi* vaccination has been associated with cognitive changes including mental confusion (17) and depressive symptoms including psychomotor retardation (11, 59). The potent effect of cytokines on cortical plasticity and cognition likely extends beyond EAE and may have wider implications in human disease.

Our findings indicate that peripheral TNF-α production plays a crucial role in synaptic instability observed in EAE mice, suggesting that blocking soluble TNF may prevent synaptic pathology and associated sensory and cognitive dysfunction. Indeed, many studies have shown that systemic or intracranial administration of anti-TNF antibodies inhibits the induction and/or progression of EAE (33, 60). It is important to note that although anti-TNF therapy is mostly beneficial for the treatment of EAE, it increases disease severity and progression in MS patients (60).

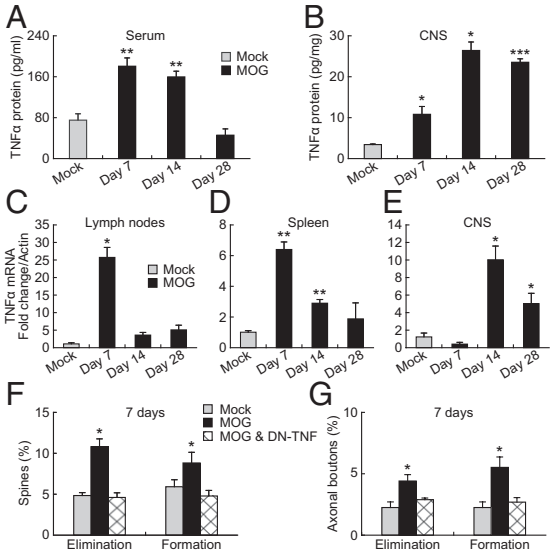

Fig. 5. Peripheral TNF-α production contributes to early synaptic instability in the cortex. (*A* and *B*) TNF-α protein levels in serum and CNS of Mock- and MOG-immunized animals. TNF-α protein level was significantly increased in both serum and CNS tissues at days 7 and 14 post-MOG immunization, but only in CNS tissues at day 28 post-MOG immunization. (*C–E*) TNF-α mRNA levels in lymph nodes, spleen, and CNS of Mock- and MOG-immunized animals. At day 7 postimmunization, a significant increase of TNF-α mRNA levels was observed in lymph nodes and spleen, but not in CNS of MOG-immunized animals compared with the Mock-immunized control. (*F*) Spine elimination and formation over 7 d after MOG immunization were significantly reduced in animals treated with DN-TNF. (*G*) Elimination and formation rates of axonal boutons over 7 d after MOG immunization were significantly reduced in animals treated with DN-TNF. Data are presented as mean ± SEM. $*P < 0.05$; $**P < 0.01$; $***P < 0.001$.

A polymorphism of multiple sclerosis in the TNFRSF1A gene, encoding for TNFR1, has been shown to mimic TNF blockade and cause a more severe clinical outcome (61). Future studies are needed to investigate the reasons for differential responses to anti-TNF therapy among EAE, MS, and other neuroinflammatory diseases. Recent studies have indicated that inhibiting TNF-α production reverses hippocampal-dependent cognitive deficits in rats injected with lipopolysaccharide (62). Additionally, a double-blind randomized controlled trial of the TNF inhibitor infliximab in patients with treatment-refractory depression shows that patients with high serum levels of inflammatory marker C-reactive protein experience relief of depressive symptoms (63). Thus, selectively targeting soluble TNF-α and preferentially preventing activation of TNFR1 and synaptic instability may serve as a potential therapeutic target to prevent cognitive symptoms in many neuroinflammatory diseases.

Materials and Methods

Experimental Animals and EAE Induction. C57BL/6J mice and mice expressing YFP in layer V pyramidal neurons (H-line) were purchased from the Jackson Laboratory. All animals were group-housed at the Skirball Institute Central Animal Facility, New York University School of Medicine. All animal experiments were approved by the Institutional Animal Care and Use Committee at New York University. For EAE induction, mice were injected s.c. with 200 μg $MOG_{35–55}$ peptide emulsified in CFA supplemented with 4 mg/mL *Mycobacterium tuberculosis* H37 RA. Each mouse received two i.p. injections (200 ng each) of pertussis toxin at days 0 and 2 postimmunization. EAE was scored as previously described (64): level 1, limp tail; level 2, hind-leg weakness or partial paralysis; level 3, total hind-leg paralysis; level 4, hind-leg paralysis and front-leg weakness or partial paralysis; level 5, moribund. For the TNF inhibitor experiment, immediately after EAE induction, mice received daily i.p. injections of XPro1595 (10 mg/kg) for 7 consecutive days.

In Vivo Transcranial Two-Photon Imaging. Dendritic spines and axonal boutons in the mouse somatosensory cortex were imaged with a two-photon microscope through a thinned-skull window. This procedure has been described in detail previously (38). In brief, YFP-H transgenic mice were deeply anesthetized with an i.p. injection of a mixture of ketamine (100 mg/kg) and xylazine (15 mg/kg). The mouse head was shaved and the skull surface was exposed with a midline incision. The region (~0.2 mm in diameter) to be imaged was identified over primary somatosensory cortex based on stereotaxic coordinates (1.1 mm posterior from bregma and 3.4 mm lateral from the midline). After removing the periosteum tissue, a custom-made steel plate was glued onto the skull to immobilize the head. To create a cranial window for imaging, a high-speed microdrill was used to remove the external layer of the compact bone and the most spongy bone. A microsurgical blade was then used to continue the thinning process until the cranial surface was ~20 μm in thickness. A high-quality picture of the brain vasculature was taken with a CCD camera mounted on the dissection microscope and used as a landmark for future relocation. Image stacks of neuronal processes within a depth of 100 μm from the pial surface were obtained with a two-photon laser tuned to 920 nm and using a 1.1 N.A. 60× water-immersion objective, yielding a full 3D data set of dendrites and axons in the area of interest. After imaging, the plate was gently detached from the skull, and the scalp was sutured with 6–0 silk. The animals were returned to their home cages until the next viewing.

Imaging Data Analysis. National Institutes of Health ImageJ software was used to analyze image stacks. The same dendritic and axonal segments were identified from 3D stacks taken from different time points with high image quality with a ratio of signal to background noise >4:1. The number and location of dendritic protrusions, defined as extensions more than one-third of dendritic shaft diameter, were identified without prior knowledge of the animal's age, interval between views, or the order of the views. The total number of spines or boutons (*n*) was pooled from dendritic or axonal segments of different animals. Filopodia were identified as long thin structures, defined as extensions larger than twice the average spine length with a ratio of head diameter to neck diameter <1.2:1 and a ratio of length to neck diameter >3:1. The remaining protrusions were classified as spines. No subtypes of spines were separated. Axonal boutons were identified as the enlarged structure along axons that are at least three times brighter than the adjacent axonal shaft. Spines or axonal boutons were considered the same between views if their positions remained the same distance from relative adjacent landmarks and were considered different if they were more than 0.7 μm away from their expected positions based on the prior view. *P* values were calculated using the Student *t* test. Differences were considered significant when $P < 0.05$.

ELISA. Mice were deeply anesthetized, and whole blood was collected by ventricular puncture. Mice were then perfused with 40 mL of Ca^{2+}/Mg^{2+}-free Dulbecco's PBS (DPBS) to remove remaining blood. Blood samples were incubated for 15 min at room temperature and then centrifuged at 1,000 × *g* for 10 min to generate serum fractions. CNS tissues were harvested and disrupted by sonication in Nonidet P-40 lysis buffer [50 mM Tris, pH 7.4, 150 mM NaCl, 1% (vol/vol) Nonidet P-40, 0.1% (vol/vol) Triton X-100, and 0.1% (wt/vol) SDS] supplemented with protease inhibitors. The homogenized material was centrifuged at 20,000 × *g* for 15 min, and the cleared supernatant was collected for analysis. Total protein levels in CNS homogenates were determined by the bicinchoninic acid assay (Pierce). TNF-α levels were measured using the Mouse TNF-α Platinum ELISA kit (eBioscience) according to the manufacturer's instructions.

Flow Cytometry. Mice were deeply anesthetized and perfused with 40 mL of Ca^{2+}/Mg^{2+}-free DPBS. It has been shown that effector T cells crawl against blood flow along the walls of meningeal vessels within 24 h of adoptive T-cell transfer in a mouse model of EAE (52). Therefore, the step of perfusing animals before homogenizing brains to assess with flow cytometry is important to remove "passenger" lymphocytes within blood vessels. The spleen and CNS tissues were removed and placed in DPBS with 2% (vol/vol) FCS. Single-cell suspensions of spleen and CNS were prepared. For CNS tissue single-cell preparation, brains were minced, and 300 U of collaganse D (Roche) was added followed by incubation at 37 °C for 30 min. Collagenase was inactivated by the addition of 12.5 mM EDTA for an additional 5-min incubation at 37 °C. Digested material was passed through a 100-μM cell strainer, followed by a continuous 38% Percoll gradient at 2,000 × *g*. The resulting CNS cell pellets and splenic suspensions were resuspended in FACS buffer. Nonspecific binding to Fc receptors was blocked by incubation with anti-CD16/32 antibody, and cells were stained with flurochrome-conjugated antibodies from eBioscience [CD4 APC-eFluor780 clone RM4-5; CD19 e450 clone eBio1D3; MHC II (I-A/I-E) e450 clone M5/11.4.15.2; CD86 APC clone GL1] and from Biolegend (CD11b PE clone M1/70; CD45 A700 clone 30-F11; CD8a PE-Cy7 clone 53-6.7; CD80 PerCP-Cy5.5 clone 16-10A1). Cytometry was performed on an LSRII (BD) and analyzed with FlowJo v 8.7 Treestar.

Immunohistochemistry. Mice were anesthetized and perfused with PBS and fixed overnight in 4% (wt/vol) paraformaldehyde at 4 °C. Tissue was rinsed three times with PBS, embedded in 2% (wt/vol) agarose, and sectioned at 150 μm with a vibratome. Sections were permeabilized in 1% (vol/vol) Titron X-100 in PBS for 3 h and blocked with 5% (vol/vol) normal goat serum for 1 h. Sections were incubated with primary antibody against Iba-1 (Wako) diluted 1:500 in blocking solution overnight, washed three times with PBS/0.05% (vol/vol) Tween-20, and then incubated with Alexafluor 555-conjugated goat anti-rabbit IgG secondary antibody 1:500 in PBS for 2 h. Sections were washed as before and mounted for imaging. Confocal images were obtained on a Bio-Rad Radiance 2000 confocal microscope. Z-projections from multiple imaging planes were generated using Image-J software. The percentage of Iba-1^+ area was calculated by making a binary image from the Z-projection and using the Image-J "analyze particle" routine.

Quantitative RT-PCR. Mice were deeply anesthetized and perfused with 40 mL of Ca^{2+}/Mg^{2+}-free DPBS. Brachial and inguinal lymph nodes, spleen, and CNS were removed from each animal and placed into TRIzol reagent (Life Technologies). Tissue was homogenized with an Omni TH tissue homogenizer, and mRNA extraction was performed according to the manufacturer's instructions. Contaminating genomic DNA was removed using the Turbo RNase-free kit (Ambion). cDNA was generated from 1 μg of total RNA using SuperScript II with random hexamers (Life Technologies). Quantitative PCR was performed on a MyIQ thermal cycler (Bio-Rad) with Maxima SYBR Green Mastermix (Fermentas). The following primers were used for PCR amplification: TNF-α (5′-TCGTAGCAAACCACCAAGTG-3′ and 5′-CCTTGAAGAGAACCTGGGAGT-3′) and β-actin (5′-GAGGCCCAGAGCAAGAGAGG-3′ and 5′- GTACTTGCGCTCAGGAGGAGC-3′).

ACKNOWLEDGMENTS. We thank Dr. David Szymkowski and Xencor Inc. for providing XPro1595 for use in this study and Dr. Juan J. Lafaille for reagents and helpful discussions. This work was supported by National Institutes of Health Grants R01 NS047325 (to W.-B.G.) and F30 MH096370 (to C.N.P.) and by research grants from American Federation for Aging Research (to G.Y.) and Alzheimer's Association (NIRG-11-205362; to G.Y.).

1. Lisak RP (2007) Neurodegeneration in multiple sclerosis: Defining the problem. *Neurology* 68(22 Suppl 3):S5–S12; discussion S43–S54.
2. Magnano I, Aiello I, Piras MR (2006) Cognitive impairment and neurophysiological correlates in MS. *J Neurol Sci* 245(1–2):117–122.
3. Mayeux R, Benson DF (1979) Phantom limb and multiple sclerosis. *Neurology* 29(5): 724–726.
4. Zarei M, Chandran S, Compston A, Hodges J (2003) Cognitive presentation of multiple sclerosis: Evidence for a cortical variant. *J Neurol Neurosurg Psychiatry* 74(7):872–877.
5. Achiron A, Barak Y (2003) Cognitive impairment in probable multiple sclerosis. *J Neurol Neurosurg Psychiatry* 74(4):443–446.
6. Lassmann H, Brück W, Lucchinetti CF (2007) The immunopathology of multiple sclerosis: An overview. *Brain Pathol* 17(2):210–218.
7. Wensky AK, et al. (2005) IFN-gamma determines distinct clinical outcomes in autoimmune encephalomyelitis. *J Immunol* 174(3):1416–1423.
8. Centonze D, et al. (2010) The link between inflammation, synaptic transmission and neurodegeneration in multiple sclerosis. *Cell Death Differ* 17(7):1083–1091.
9. Hofstetter HH, et al. (2005) The cytokine signature of MOG-specific CD4 cells in the EAE of C57BL/6 mice. *J Neuroimmunol* 170(1–2):105–114.
10. Brambilla R, et al. (2011) Inhibition of soluble tumour necrosis factor is therapeutic in experimental autoimmune encephalomyelitis and promotes axon preservation and remyelination. *Brain* 134(Pt 9):2736–2754.
11. Baune BT, et al. (2012) Tumour necrosis factor-alpha mediated mechanisms of cognitive dysfunction. *Transl Neurosci* 3(3):263–277.
12. Gendron RL, Nestel FP, Lapp WS, Baines MG (1991) Expression of tumor necrosis factor alpha in the developing nervous system. *Int J Neurosci* 60(1–2):129–136.
13. Kaneko M, Stellwagen D, Malenka RC, Stryker MP (2008) Tumor necrosis factor-alpha mediates one component of competitive, experience-dependent plasticity in developing visual cortex. *Neuron* 58(5):673–680.
14. Khairova RA, Machado-Vieira R, Du J, Manji HK (2009) A potential role for pro-inflammatory cytokines in regulating synaptic plasticity in major depressive disorder. *Int J Neuropsychopharmacol* 12(4):561–578.
15. Leonoudakis D, Braithwaite SP, Beattie MS, Beattie EC (2004) TNFalpha-induced AMPA-receptor trafficking in CNS neurons: Relevance to excitotoxicity? *Neuron Glia Biol* 1(3):263–273.
16. McCoy MK, Tansey MG (2008) TNF signaling inhibition in the CNS: Implications for normal brain function and neurodegenerative disease. *J Neuroinflammation* 5(1):45.
17. Reichenberg A, et al. (2001) Cytokine-associated emotional and cognitive disturbances in humans. *Arch Gen Psychiatry* 58(5):445–452.
18. Sriram K, O'Callaghan JP (2007) Divergent roles for tumor necrosis factor-α in the brain. *J Neuroimmune Pharmacol* 2(2):140–153.
19. Centonze D, et al. (2009) Inflammation triggers synaptic alteration and degeneration in experimental autoimmune encephalomyelitis. *J Neurosci* 29(11):3442–3452.
20. Javed A, Arnason BGW (2009) Demyelinating diseases. *Encyclopedia of Neuroscience*, ed Larry RS (Academic Press, New York), pp 415–422.
21. Peruga I, et al. (2011) Inflammation modulates anxiety in an animal model of multiple sclerosis. *Behav Brain Res* 220(1):20–29.
22. Ransohoff RM, Kivisäkk P, Kidd G (2003) Three or more routes for leukocyte migration into the central nervous system. *Nat Rev Immunol* 3(7):569–581.
23. Kim JV, et al. (2010) Two-photon laser scanning microscopy imaging of intact spinal cord and cerebral cortex reveals requirement for CXCR6 and neuroinflammation in immune cell infiltration of cortical injury sites. *J Immunol Methods* 352(1–2):89–100.
24. Hickey WF, Hsu BL, Kimura H (1991) T-lymphocyte entry into the central nervous system. *J Neurosci Res* 28(2):254–260.
25. Pollak Y, Ovadia H, Orion E, Weidenfeld J, Yirmiya R (2003) The EAE-associated behavioral syndrome: I. Temporal correlation with inflammatory mediators. *J Neuroimmunol* 137(1–2):94–99.
26. Gutierrez EG, Banks WA, Kastin AJ (1993) Murine tumor necrosis factor alpha is transported from blood to brain in the mouse. *J Neuroimmunol* 47(2):169–176.
27. Pan WH, Banks WA, Kennedy MK, Gutierrez EG, Kastin AJ (1996) Differential permeability of the BBB in acute EAE: Enhanced transport of TNF-alpha. *Am J Physiol-Endoc M* 271(4):E636–E642.
28. Pan W, Kastin AJ (2002) TNFalpha transport across the blood-brain barrier is abolished in receptor knockout mice. *Exp Neurol* 174(2):193–200.
29. Boettger MK, Weishaupt A, Geis C, Toyka KV, Sommer C (2010) Mild experimental autoimmune encephalitis as a tool to induce blood-brain barrier dysfunction. *J Neural Transm* 117(2):165–169.
30. Stellwagen D, Malenka RC (2006) Synaptic scaling mediated by glial TNF-alpha. *Nature* 440(7087):1054–1059.
31. Stellwagen D, Beattie EC, Seo JY, Malenka RC (2005) Differential regulation of AMPA receptor and GABA receptor trafficking by tumor necrosis factor-alpha. *J Neurosci* 25(12):3219–3228.
32. Beattie EC, et al. (2002) Control of synaptic strength by glial TNFalpha. *Science* 295(5563):2282–2285.
33. Baker D, et al. (1994) Control of established experimental allergic encephalomyelitis by inhibition of tumor necrosis factor (TNF) activity within the central nervous system using monoclonal antibodies and TNF receptor-immunoglobulin fusion proteins. *Eur J Immunol* 24(9):2040–2048.
34. Probert L, et al. (2000) TNFR1 signalling is critical for the development of demyelination and the limitation of T-cell responses during immune-mediated CNS disease. *Brain* 123(Pt 10):2005–2019.
35. Zalevsky J, et al. (2007) Dominant-negative inhibitors of soluble TNF attenuate experimental arthritis without suppressing innate immunity to infection. *J Immunol* 179(3):1872–1883.
36. Steed PM, et al. (2003) Inactivation of TNF signaling by rationally designed dominant-negative TNF variants. *Science* 301(5641):1895–1898.
37. Grutzendler J, Kasthuri N, Gan WB (2002) Long-term dendritic spine stability in the adult cortex. *Nature* 420(6917):812–816.
38. Yang G, Pan F, Parkhurst CN, Grutzendler J, Gan WB (2010) Thinned-skull cranial window technique for long-term imaging of the cortex in live mice. *Nat Protoc* 5(2): 201–208.
39. Yang G, Pan F, Gan WB (2009) Stably maintained dendritic spines are associated with lifelong memories. *Nature* 462(7275):920–924.
40. Shepherd GM, Harris KM (1998) Three-dimensional structure and composition of CA3→CA1 axons in rat hippocampal slices: Implications for presynaptic connectivity and compartmentalization. *J Neurosci* 18(20):8300–8310.
41. Brown DA, Sawchenko PE (2007) Time course and distribution of inflammatory and neurodegenerative events suggest structural bases for the pathogenesis of experimental autoimmune encephalomyelitis. *J Comp Neurol* 502(2):236–260.
42. Goverman J (2009) Autoimmune T cell responses in the central nervous system. *Nat Rev Immunol* 9(6):393–407.
43. Lichtman JW, Colman H (2000) Synapse elimination and indelible memory. *Neuron* 25(2):269–278.
44. Bailey CH, Kandel ER (1993) Structural changes accompanying memory storage. *Annu Rev Physiol* 55:397–426.
45. Staffen W, et al. (2002) Cognitive function and fMRI in patients with multiple sclerosis: Evidence for compensatory cortical activation during an attention task. *Brain* 125(Pt 6):1275–1282.
46. Bø L, Vedeler CA, Nyland H, Trapp BD, Mørk SJ (2003) Intracortical multiple sclerosis lesions are not associated with increased lymphocyte infiltration. *Mult Scler* 9(4): 323–331.
47. Gutierrez H, Davies AM (2011) Regulation of neural process growth, elaboration and structural plasticity by NF-κB. *Trends Neurosci* 34(6):316–325.
48. Saha RN, Liu X, Pahan K (2006) Up-regulation of BDNF in astrocytes by TNF-alpha: A case for the neuroprotective role of cytokine. *J Neuroimmune Pharmacol* 1(3): 212–222.
49. Horch HW, Krüttgen A, Portbury SD, Katz LC (1999) Destabilization of cortical dendrites and spines by BDNF. *Neuron* 23(2):353–364.
50. Aloe L, et al. (1999) Learning abilities, NGF and BDNF brain levels in two lines of TNF-alpha transgenic mice, one characterized by neurological disorders, the other phenotypically normal. *Brain Res* 840(1):125–137.
51. Kerschensteiner M, Meinl E, Hohlfeld R (2009) Neuro-immune crosstalk in CNS diseases. *Neuroscience* 158(3):1122–1132.
52. Bartholomäus I, et al. (2009) Effector T cell interactions with meningeal vascular structures in nascent autoimmune CNS lesions. *Nature* 462(7269):94–98.
53. Gimenez MA, Sim JE, Russell JH (2004) TNFR1-dependent VCAM-1 expression by astrocytes exposes the CNS to destructive inflammation. *J Neuroimmunol* 151(1–2): 116–125.
54. Miller AH, Maletic V, Raison CL (2009) Inflammation and its discontents: The role of cytokines in the pathophysiology of major depression. *Biol Psychiatry* 65(9):732–741.
55. Stigler KA, Sweeten TL, Posey DJ, McDougle CJ (2009) Autism and immune factors: A comprehensive review. *Res Autism Spectr Disord* 3(4):840–860.
56. Di Filippo M, Sarchielli P, Picconi B, Calabresi P (2008) Neuroinflammation and synaptic plasticity: Theoretical basis for a novel, immune-centred, therapeutic approach to neurological disorders. *Trends Pharmacol Sci* 29(8):402–412.
57. Terrando N, et al. (2010) Tumor necrosis factor-alpha triggers a cytokine cascade yielding postoperative cognitive decline. *Proc Natl Acad Sci USA* 107(47):20518–20522.
58. Holmes C (2013) Review: Systemic inflammation and Alzheimer's disease. *Neuropathol Appl Neurobiol* 39(1):51–68.
59. Brydon L, Harrison NA, Walker C, Steptoe A, Critchley HD (2008) Peripheral inflammation is associated with altered substantia nigra activity and psychomotor slowing in humans. *Biol Psychiatry* 63(11):1022–1029.
60. Lim SY, Constantinescu CS (2010) TNF-α: A paradigm of paradox and complexity in multiple sclerosis and its animal models. *Open Autoimmun J* 2:160–170.
61. Gregory AP, et al. (2012) TNF receptor 1 genetic risk mirrors outcome of anti-TNF therapy in multiple sclerosis. *Nature* 488(7412):508–511.
62. Belarbi K, et al. (2012) TNF-alpha protein synthesis inhibitor restores neuronal function and reverses cognitive deficits induced by chronic neuroinflammation. *J Neuroinflammation* 9:23.
63. Raison CL, et al. (2013) A randomized controlled trial of the tumor necrosis factor antagonist infliximab for treatment-resistant depression: The role of baseline inflammatory biomarkers. *JAMA Psychiatry* 70(1):31–41.
64. Baron JL, Madri JA, Ruddle NH, Hashim G, Janeway CA, Jr. (1993) Surface expression of alpha 4 integrin by CD4 T cells is required for their entry into brain parenchyma. *J Exp Med* 177(1):57–68.